J Mol Model (2013) 19:4181–4193
DOI 10.1007/s00894-013-1779-y

ORIGINAL PAPER

Theoretical study of the kinetics of chlorine atom abstraction from chloromethanes by atomic chlorine

Katarzyna Brudnik · Maria Twarda · Dariusz Sarzyński · Jerzy T. Jodkowski

Received: 31 October 2012 / Accepted: 21 January 2013 / Published online: 2 March 2013

Abstract Ab initio calculations at the G3 level were used in a theoretical description of the kinetics and mechanism of the chlorine abstraction reactions from mono-, di-, tri- and tetrachloromethane by chlorine atoms. The calculated profiles of the potential energy surface of the reaction systems show that the mechanism of the studied reactions is complex and the Cl-abstraction proceeds via the formation of intermediate complexes. The multi-step reaction mechanism consists of two elementary steps in the case of CCl_4+Cl, and three for the other reactions. Rate constants were calculated using the theoretical method based on the RRKM theory and the simplified version of the statistical adiabatic channel model. The temperature dependencies of the calculated rate constants can be expressed, in temperature range of 200–3,000 K as

$$k(CH_3Cl + Cl) = 2.08 \times 10^{-11} \times (T/300)^{1.63} \times \exp(-12780/T)\ cm^3molecule^{-1}s^{-1}$$
$$k(CH_2Cl_2 + Cl) = 2.36 \times 10^{-11} \times (T/300)^{1.23} \times \exp(-10960/T)\ cm^3molecule^{-1}s^{-1}$$
$$k(CHCl_3 + Cl) = 5.28 \times 10^{-11} \times (T/300)^{0.97} \times \exp(-9200/T)\ cm^3molecule^{-1}s^{-1}$$
$$k(CCl_4 + Cl) = 1.51 \times 10^{-10} \times (T/300)^{0.58} \times \exp(-7790/T)\ cm^3molecule^{-1}s^{-1}$$

The rate constants for the reverse reactions $CH_3/CH_2Cl/CHCl_2/CCl_3+Cl_2$ were calculated via the equilibrium constants derived theoretically. The kinetic equations

$$k(CH_3 + Cl_2) = 6.70 \times 10^{-13} \times (T/300)^{1.51} \times \exp(270/T)\ cm^3molecule^{-1}s^{-1}$$
$$k(CH_2Cl + Cl_2) = 7.34 \times 10^{-14} \times (T/300)^{1.43} \times \exp(390/T)\ cm^3molecule^{-1}s^{-1}$$
$$k(CHCl_2 + Cl_2) = 6.81 \times 10^{-14} \times (T/300)^{1.60} \times \exp(-370/T)\ cm^3molecule^{-1}s^{-1}$$
$$k(CCl_3 + Cl_2) = 1.43 \times 10^{-13} \times (T/300)^{1.52} \times \exp(-550/T)\ cm^3molecule^{-1}s^{-1}$$

allow a very good description of the reaction kinetics. The derived expressions are a substantial supplement to the kinetic data necessary to describe and model the complex gas-phase reactions of importance in combustion and atmospheric chemistry.

Keywords Chemical kinetics · Gas-phase reactions · Reaction mechanism · Chlorine abstraction · Chloromethanes

K. Brudnik · M. Twarda · D. Sarzyński · J. T. Jodkowski (✉)
Department of Physical Chemistry, Wroclaw Medical University,
pl. Nankiera 1,
50-140 Wroclaw, Poland
e-mail: jerzy.jodkowski@am.wroc.pl

K. Brudnik
e-mail: katarzyna.brudnik@umed.wroc.pl

Introduction

Chlorinated alkanes are used widely in laboratory syntheses and in the chemical industry [1]. As a consequence, they are penetrating into the environment in steadily increasing amounts. Chloroalkanes and products of their environmental reactions are considered toxic and biocumulative species. The chemical inertness and high volatility of chloromethanes mean that they can remain in the atmosphere for a very long time. The products of the atmospheric destruction of chloromethanes have been proven to have a significant impact on chlorine chemistry in the atmosphere and may be involved in various catalytic reaction cycles responsible for the depletion of the stratospheric ozone layer [1, 2].

Monochloromethane (CH_3Cl) is regarded as the most abundant halocarbon in the troposphere, and the largest natural source of stratospheric chlorine [1, 3]. The variability of CH_3Cl in the ice core over the last two millennia suggests a relationship between the concentration of atmospheric CH_3Cl and global mean temperature, which indicates the possibility that a warmer future climate may result in higher tropospheric CH_3Cl levels. Major sources of

CH_3Cl are biomass burning, oceanic emissions and vegetative emissions. The other chloromethanes occurring in polluted atmosphere, i.e., dichloromethane (CH_2Cl_2), trichloromethane ($CHCl_3$) and tetrachloromethane (CCl_4), are released primarily from industrial processes [1–5].

The reaction with hydroxyl radical is a major loss pathway for atmospheric chloromethanes. The reactions of Cl atoms with many haloalkanes can also become of some importance because the rate constants for these reactions are distinctly higher than those for the corresponding reactions with OH radicals. Therefore, in the marine boundary layer and in polar regions where the concentration of chlorine atoms is significant, Cl-initiated reactions may play a key role in the decay of many organic compounds in the troposphere.

The sources of chlorine atoms are the photochemically labile chlorine compounds such as Cl_2 and $ClNO_2$ produced in some aqueous-phase reactions in airborne seawater droplets [1, 2]. Chlorine atoms and their oxides are highly reactive species and can profoundly affect atmospheric composition. The gas-phase reactions of chlorine atoms with the hydrogen-containing atmospheric halocarbons lead to the facile generation of the corresponding free radicals via hydrogen atom abstraction. These reactions also play an important role in the processes of industrial chlorination and incineration of hazardous halogenated wastes, and their kinetics have been the subject of many theoretical and experimental studies [6–8]. Considerably less recognized are the kinetics of chlorine abstraction reactions. To the best of our knowledge, these reactions have not been investigated experimentally. In this study, we present a theoretical analysis of the mechanism and kinetics of the reactions of chloromethanes, $CH_{4-x}Cl_x$ (x=1,2,3 and 4) with atomic chlorine:

$$CH_{4-x}Cl_x + Cl \rightarrow CH_{4-x}Cl_{x-1} + Cl_2 \qquad (1)$$

Kinetic information on the reactions indicated in Eq. (1) is very limited. Chlorine abstraction reactions proceed incomparably slower than the analogous H-abstraction processes, and grow in importance only at high temperatures. The kinetics of the reverse processes

$$CH_{4-x}Cl_{x-1} + Cl_2 \rightarrow CH_{4-x}Cl_x + Cl \qquad (-1)$$

between chloromethyl radicals and molecular chlorine is considerably better known [6–8]. The reactions indicated in Eq. (−1) indeed also represent chlorine abstraction processes; however, Cl atoms in a molecule of Cl_2 are bound distinctly weaker in comparison with those in chloromethane. In consequence, the reverse reactions (Eq. −1) are relatively fast processes at ambient temperature and their kinetics have been studied experimentally over a wide temperature range, allowing comparison of experimental results with the theoretical kinetic results obtained in this study.

Computational details

It is well known that the G2 method [9] well reproduces the structural parameters and molecular properties of a wide group of organic compounds. The haloalkanes were studied theoretically using quantum mechanical ab initio methods at various levels of theory. Reliable values relating to thermochemical properties and vibrational frequencies have been obtained using G2 methodology for perhalogenated methanols, methyl hypohalites, halogenated alkyl and alkoxy radicals [10–20]. The G2 method was also used successfully in the theoretical description of the kinetics and mechanism of the abstraction of hydrogen from methanol by halogen atoms [21–23]. We decided to use the G3 method [24] in our investigations. This method provides the same quality of computational results but with a considerable reduction in the time and the levels of calculations required in comparison with the G2 method. All quantum mechanical ab initio calculations were carried out using the Gaussian 09 program package [25]. The geometries of all stationary point structures of the potential energy surface were fully optimized at both the SCF and MP2 levels with the 6–31G(d) basis set. Relative total energies were examined using G3 methodology [24].

The rate constants of the reactions studied were analyzed in terms of conventional transition state theory (TST) [26, 27] according to the equation

$$k_{TST} = \kappa_T \sigma \frac{k_B T}{h} \exp\left(\frac{\Delta S^{\neq}}{R}\right) \exp\left(-\frac{\Delta H^{\neq}}{RT}\right) \qquad (2)$$

where κ_T is the tunneling correction factor, σ denotes a symmetry factor related to degeneracy of the reaction path, and k_B and h are the Boltzmann and Planck constants, respectively. $\Delta S^{\neq}$ is the activation entropy and $\Delta H^{\neq}$ the activation enthalpy of the reaction under investigation. Values of κ_T were evaluated from the simple Wigner's expression [26]

$$\kappa_T \cong 1 - \frac{1}{24}\left(\frac{h\nu^{\neq}}{k_B T}\right)^2 \qquad (3)$$

with the imaginary frequencies $\nu^{\neq}$ of the transition state obtained in the geometry optimization performed at a higher level of theory, i.e., from MP2/6–31G(d) calculations. The vibrational and rotational contributions to the thermodynamic functions were derived by classical harmonic-oscillator rigid-rotor approximation (no free or internal rotation was considered).

Results and discussion

The theoretical investigation of hydrogen abstraction from halomethanes by chlorine atoms shows that the mechanism of these reactions appears to be complex and consists of some consecutive elementary processes with the formation of loosely bound intermediate complexes [21–23]. Therefore, at each level of theory, the potential energy surface of the studied reactions was explored for the possible existence of transition states and intermediate complexes. The geometries of all structures were optimized fully and independently using analytical gradients at the SCF and MP2 levels with the 6–31G(d) basis set. The molecular arrangements and definitions of the structural parameters of the molecular structures taking part in the mechanism of reactions $CH_{4-x}Cl_x+Cl$ (x=1,2,3 and 4) are shown in Fig. 1. The results of calculations including the geometrical parameters optimized at the MP2/6–31G(d) level, the harmonic vibrational frequencies, the rotational constants and the total G3(0 K) energies (ZPE included) for the reactants, products, intermediate complexes and transition states are given in Tables 1 and 2.

Optimized molecular structures

The reactants are highly symmetrical molecular structures. A symmetry of point groups of C_{3v}, C_{2v}, C_{3v} and T_D is found for CH_3Cl, CH_2Cl_2, $CHCl_3$ and CCl_4, respectively. The C–H and C–Cl bond lengths obtained in the geometry optimization performed at the MP2(Full)/6–31G(d) level for reactants are very close one to another. The lengths of C–Cl bonds in chloromethanes are within 1.765–1.777 Å whereas C–H bonds cover a narrow range of 1.086–1.088 Å. The differences in the values of the angular parameters, H–C–H and Cl–C–H in the reactants do not exceed 1°.

The radical products of the reactions under investigation show more visible differences in structural parameters. Methyl radical (CH_3) is a planar structure with the symmetry of a D_{3h} point group. Trichloromethyl radical (CCl_3) is also a highly symmetrical structure with a three-fold axis. The equilibrium geometry of CCl_3 radical obtained at the MP2/6–31G(d) level corresponds to a C_{3v} symmetry. The other radicals, chloromethyl (CH_2Cl) and dichloromethyl ($CHCl_2$) are less symmetrical molecular structures. Either the C–H or the C–Cl bonds in the radical products are a little shorter than their counterparts in the parent chloromethanes.

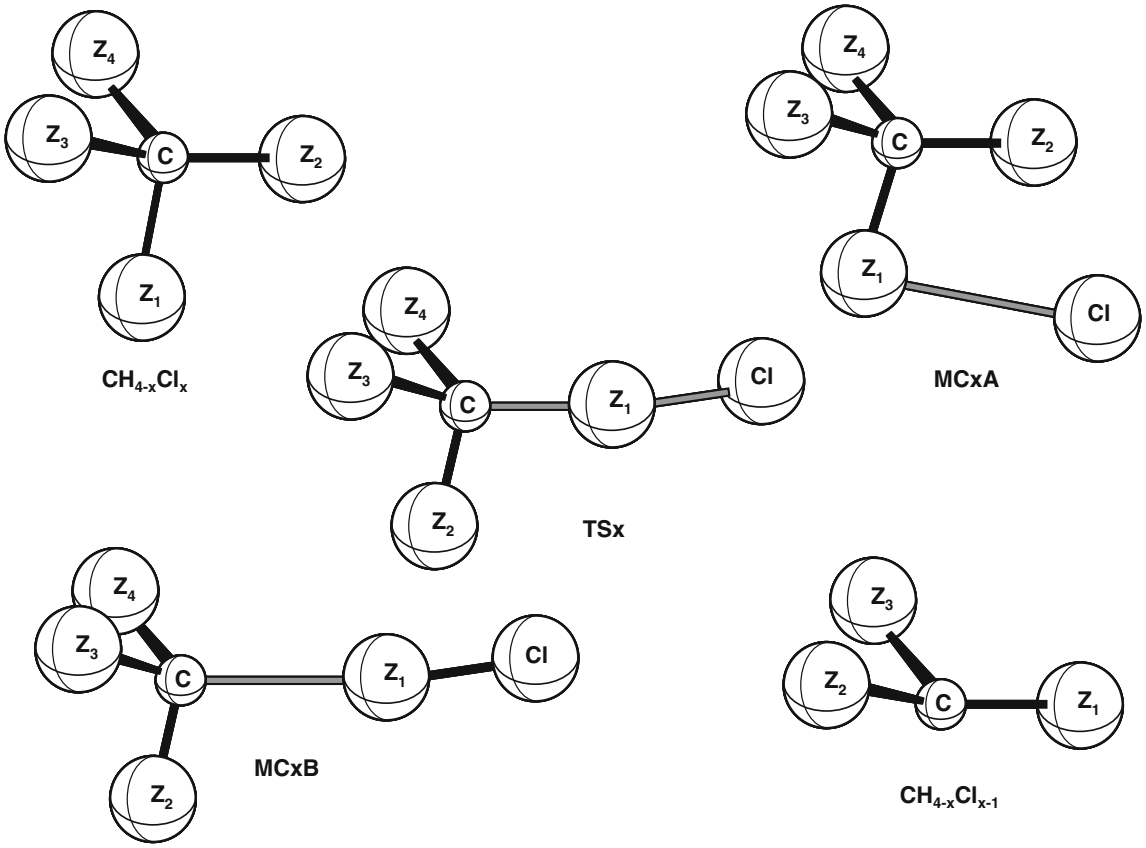

Fig. 1 Definition of the geometrical parameters of molecular structures taking part in the mechanism of reaction of atomic chlorine with CH_3Cl, CH_2Cl_2, $CHCl_3$ and CCl_4; *Z* denotes H or Cl atoms, and *x*=1, 2, 3 or 4

In contrast, the values of the angular parameters in radical products, Cl–C–H and H–C–H are distinctly greater than those in the corresponding reactants.

Except for tetrachloromethane, the attack of a chlorine atom on molecules of CH_3Cl, CH_2Cl_2 and $CHCl_3$ leads to the formation of the pre-reaction adducts, $CH_{4-x}Cl_x$…Cl (x=1,2 and 3) denoted by MC1A, MC2A and MC3A for CH_3Cl…Cl, CH_2Cl_2…Cl and $CHCl_3$…Cl, respectively. The adducts MC1A and MC3A have a C_s symmetry, because the attacking chlorine atom is moving across the symmetry plane of the CH_3Cl or $CHCl_3$. The geometrical parameters of these molecular complexes retain the values that appear in the isolated reactants. All pre-reaction adducts, CH_3Cl…Cl, CH_2Cl_2…Cl and $CHCl_3$…Cl, are loose molecular structures with long contact distances between the attacking chlorine and reactant. The vibrational frequencies of MC1A, MC2A and

Table 1 Molecular properties of the reactants and products of the reactions under investigation calculated at the G3 level[a]. The vibrational frequencies ν_i (cm^{-1}) obtained at the SCF/6–31G(d) level and scaled by 0.8929 (first column), derived in the MP2(full)/6–31G(d) calculations (second column) were scaled by 0.94 for reactants and products. Experimental frequencies [28–32] are given in parenthesis

	CH_3Cl (C_{3v})			CH_2Cl_2 (C_{2v})			$CHCl_3$ (C_{3v})			CCl_4 (T_D)		
C–Cl	1.7770			1.7673			1.7648			1.7688		
C–H	1.0877			1.0869			1.0859					
H–C–Cl	108.9063			108.2652			107.6497					
Cl–C–Cl				113.0095			111.2297			109.4712		
H–C–H	110.0290			110.7900								
A	157.84728			32.625180			3.284360			1.732250		
B	13.37535			3.291950			3.284350			1.732250		
C	13.37530			3.048430			1.703430			1.732250		
ν_1	700	739	(732)	278	283	(282)	258	261	(261)	218	220	(217)
ν_2	1,016	1,020	(1,017)	691	709	(717)	258	261	(261)	218	220	(217)
ν_3	1,016	1,020	(1,017)	752	768	(758)	360	364	(363)	311	315	(314)
ν_4	1,374	1,380	(1,355)	889	894	(898)	652	664	(680)	311	315	(314)
ν_5	1,454	1,453	(1,452)	1,174	1,172	(1,153)	780	774	(774)	311	315	(314)
ν_6	1,454	1,453	(1,452)	1,295	1,295	(1,268)	780	774	(774)	449	452	(459)
ν_7	2,917	2,965	(2,937)	1,445	1,438	(1,467)	1,249	1,238	(1,220)	806	783	(776)
ν_8	3,009	3,071	(3,039)	2,980	3,002	(2,999)	1,249	1,238	(1,220)	806	783	(776)
ν_9	3,009	3,071	(3,039)	3,053	3,079	(3,040)	3,043	3,047	(3,034)	806	783	(776)
E_0(G3)	−499.91251			−959.37103			−1,418.82886			−1,878.28323		

	CH_3 (D_{3h})			CH_2Cl (C_s)			$CHCl_2$ (C_s)			CCl_3 (C_{3v})		
C-Cl				1.7007			1.7029			1.7109		
C-H	1.0783			1.0780			1.0809					
H-C-Cl				117.4525			116.591					
Cl-C-Cl							119.0484			116.887		
H-C-H	120.0000			122.8962								
A	287.529180			275.216580			47.036420			3.377060		
B	287.529180			15.849680			3.350770			3.377030		
C	143.764590			15.012400			3.135160			1.699920		
ν_1	275	380		441	313	(389)	290	302	(190±50)	264	273	(290)
ν_2	1,375	1,392	(1,428)	777	831	(829)	542	526		264	273	(290)
ν_3	1,375	1,392	(1,428)	976	995		721	753	(845)	313	345	
ν_4	2,933	3,028	(2,931)	1,381	1,407	(1,391)	863	891	(896)	484	494	(509)
ν_5	3,090	3,206	(3,087)	2,996	3,074	(3,055)	1,228	1,247	(1,226)	894	896	(898)
ν_6	3,090	3,206	(3,087)	3,127	3,215		3,063	3,113		894	896	(898)
E_0(G3)	−39.79223			−499.25600			−958.71926			−1,418.18095		

[a] G3 molecular parameters: geometrical structure optimized at the MP2(Full)/6–31 G(d) level, (bond lengths in Å, valence and dihedral angles in degrees), rotational constants ABC in GHz, the total G3-energies in a.u. at 0 K (ZPE included)

Table 2 Molecular properties of structures taking part in the mechanism of reaction under investigation derived at the G3 level [a]

	MC1A (C_s)	TS1 (C_{3v})	MC1B (C_{3v})	MC2A	TS2 (C_s)	MC2B (C_s)	MC3A (C_s)	TS3 (C_s)	MC3B (C_s)	TS4 (C_{3v})	MC4B (C_{3v})
$ClCl_0$	3.1706	2.0952	2.0232	5.1473	2.1118	2.0232	3.4875	2.1344	2.0222	2.1589	2.0204
CCl_0	1.7794	2.3218	3.0624	1.7675	2.2707	3.0366	1.7682	2.2175	3.0234	2.1747	3.0465
CH_1	1.0880	1.0810	1.0791								
CCl_1				1.7675	1.6944	1.6989	1.7634	1.7036	1.7014	1.7198	1.7104
CH_2	1.0879	1.0810	1.0791	1.0866	1.0822	1.0793					
CCl_2							1.7634	1.7036	1.7014	1.7198	1.7104
CH_3	1.0879	1.0810	1.0791	1.0866	1.0822	1.0793	1.0857	1.0841	1.0818		
CCl_3										1.7198	1.7104
ClH_3	3.6039			3.3509			2.9519				
$ClCl_0C$	92.418	180.000	180.000	56.503	176.405	177.145	83.245	177.0693	176.702	180.000	180.000
H_1CCl_0	108.622	98.310	93.025								
Cl_1CCl_0				112.976	109.557	107.229	111.111	106.6787	104.644	104.013	100.491
H_2CCl_0	108.761	98.310	93.025	108.277	96.591	91.559					
Cl_2CCl_0							111.111	106.6787	104.644	104.013	100.491
H_3CCl_0	108.761	98.310	93.025	108.277	96.591	91.559	107.289	94.7909	89.021		
Cl_3CCl_0										104.013	100.491
ClH_3C				169.799			128.005				
H_1CCl_0Cl	180.000										
Cl_1CCl_0Cl				113.208	180.000	180.0	117.718	117.0209	117.052		
H_2CCl_0Cl	60.339			−126.932	119.938	61.020					
Cl_2CCl_0Cl							−117.718	−117.0209	−117.052		
H_3CCl_0Cl	−60.339			−6.705	−119.938	−61.020	0.000	0.000	0.000		
Cl_3CCl_0Cl											
A	14.037520	146.090730	143.959080	3.127490	18.545620	17.885810	2.114150	3.241100	3.192540	1.730210	1.703120
B	2.283420	2.280780	1.806480	0.851610	0.957270	0.744410	0.834620	0.807110	0.607000	0.627540	0.484290
C	1.988730	2.280780	1.806480	0.687030	0.916060	0.718320	0.762120	0.659880	0.518380	0.627540	0.484290
ν_1	29	471i	53	5	501i	25	7	552i	24	612i	26
ν_2	46	72	53	8	59	49	26	44	32	8	26
ν_3	67	72	81	10	73	56	47	56	53	8	46
ν_4	733	360	150	283	146	89	261	148	53	150	46
ν_5	1,023	515	150	709	360	160	261	168	108	150	47
ν_6	1,023	515	513	768	551	509	365	320	304	190	274
ν_7	1,379	944	524	893	818	526	664	386	506	286	274
ν_8	1,451	1,396	1,392	1,171	955	834	769	712	584	286	360
ν_9	1,451	1,396	1,392	1,293	1,030	1,001	776	872	758	414	505
ν_{10}	2,964	3,011	3,023	1,437	1,411	1,407	1,239	928	890	545	505
ν_{11}	3,072	3,184	3,200	3,002	3,043	3,063	1,242	1,249	1,247	858	894
ν_{12}	3,072	3,184	3,200	3,079	3,171	3,201	3,053	3,083	3,105	858	894
$E_0(G3)$ [b]	−15.15	105.88	100.66	−3.31	89.86	84.85	−6.72	75.07	66.99	62.15	44.90

[a] G3 molecular parameters: geometrical structure optimized at the MP2(Full)/6–31G(d) level, (bond lengths in Å, valence and dihedral angles in degrees), rotational constants ABC in GHz, the vibrational frequencies ν_i (cm^{-1}) obtained at the MP2/6–31G(d) level and scaled by 0.940

[b] The total G3-energies in $kJmol^{-1}$ at 0 K (ZPE included) calculated towards the G3-energy of the respective reactants' energy

MC3A from ν_4 up are almost identical with the corresponding frequencies in the isolated reactants.

The transition states $(CH_{4-x}Cl_{x-1}\ldots Cl\ldots Cl)^{\neq}$, denoted by TSx (x=1,2,3 and 4) describe the chlorine abstraction from $CH_{4-x}Cl_x$ by Cl atom. All transition states are reactant-like structures. In reactions CH_3Cl+Cl and CCl_4+Cl, the attacking Cl atom is approaching CH_3Cl and CCl_4 along the C–Cl_0 bond. The angle of C–Cl_0–Cl is then equal to 180° and the three-fold axis of the reactant molecule (CH_3Cl or CCl_4) is retained in the structure of transition states TS1 and TS4, which have the symmetry of a C_{3v} point group. Both TS2 and TS3 are molecular structures with the C–Cl_0/Cl_0–Cl bonds breaking/formed located in the symmetry plane of the transition state. The attack of the chlorine atom at the TS2 and TS3 structures is nearly collinear, with values of the angle C–Cl_0–Cl of 177° and 176° found for TS2 and TS3, respectively. The calculated lengths of the breaking bonds C–Cl_0 are 30 % longer than those in the parent reactants. The length of C–Cl_0 decreases with the increase in the number of chlorine atoms in the reactant molecule. The Cl_0–Cl bonds formed are only 4–7 % longer than the Cl–Cl bond in molecular chlorine. The values of the other structural parameters of the transition states TSx are close to their counterparts in the isolated reactants.

The post-reaction adducts, $CH_{4-x}Cl_{x-1}\ldots Cl_2$, designated by MCxB (x=1,2,3 and 4), are intermediates consisting of two subunits: radical $CH_{4-x}Cl_{x-1}$ and molecular chlorine Cl_2, bonded in a molecular complex. All molecular complexes, MCxB keep the symmetry of their respective transition states TSx, so that MC1B and MC4B have a C_{3v} symmetry whereas MC2B and MC3B possess a C_s symmetry. The vibrational frequencies of these adducts are very close to the corresponding frequencies in the isolated radical product and Cl_2.

In standard G3 approach, the vibrational frequencies are obtained in geometry optimization performed at the SCF/6–31G(d) level and scaled by 0.8929 to take into account their overestimation [24]. The vibrational frequencies derived in this way reproduce the experimental frequencies well and give a correct estimation of the zero-point energy of the reactants and products. However, the optimized structures for either intermediate complexes or transition states derived at the SCF and MP2 levels shows substantial differences in both geometrical parameters and vibrational frequencies. Therefore, our kinetic analysis of the studied reactions was based on the MP2(Full)/6–31G(d)-frequencies as the more credible ones. The value of the scaling factor for the MP2-frequencies was found by comparing the available experimental [28–33] and calculated MP2 frequencies for reactants and products. As can be seen from Table 1, using a value of the scaling factor of 0.940 leads to the best agreement of the MP2 and experimental frequencies [28–33]. Therefore, this scaling factor was used to calculate the vibrational frequencies of all molecular structures taking part in the mechanism of the studied reactions.

Reaction energetics

The G3 method allows reliable estimation of the reaction energetics. The accuracy of these estimations based on the G3-energies is usually considered to be better than 6 kJ mol^{-1}. The enthalpy of formation, $\Delta H^0_{f,298}$ can be evaluated directly as the G3 enthalpy of the formation reaction of CH_xCl_y from the elemental reference compounds such as $C_{(g)}$, $H_{2(g)}$ and $Cl_{2(g)}$, i.e., $C_{(g)}+(x/2)H_{2(g)}+(y/2)Cl_{2(g)}\rightarrow CH_xCl_y$, and taking into account that the elemental standard state of carbon is graphite. An alternative approach involved the total G3-energy for the atomization reaction $CH_xCl_y \rightarrow C_{(g)}+xH_{(g)}+yCl_{(g)}$ in combination with the calculated and experimental values of the enthalpy of formation of the gaseous atoms, such as $\Delta H^0_{f,298}\left(C_{(g)}\right) = 716.7$ kJ mol^{-1}, $\Delta H^0_{f,298}\left(H_{(g)}\right) = 218.0$ kJ mol^{-1} and $\Delta H^0_{f,298}\left(Cl_{(g)}\right) = 121.3$ kJ mol^{-1} [6, 7].

Table 3 compares the values of $\Delta H^0_{f,298}$ of the reactants and products of the studied reactions derived on the basis of the total G3-energy calculated for the formation of CH_xCl_y (a) or for its atomization reaction (b). The results presented show that the calculated values of $\Delta H^0_{f,298}$ in both approaches (a) and (b) are in very good agreement with the experimental estimates for CH_3Cl, CH_2Cl_2, CH_3 and CH_2Cl. However, the heat of reaction $½Cl_2\rightarrow Cl$ calculated at the G3 level is associated with an error of 2.4 kJmol^{-1} at 298 K with respect to the experimental estimate. This is the primary cause of the sizable errors in the values of $\Delta H^0_{f,298}$ calculated by the formation of CH_xCl_y for molecular structures containing three or more chlorine atoms. The calculations of $\Delta H^0_{f,298}$ for CH_xCl_y (y>2) on the basis of the G3-energy for the atomization reaction reproduce the experimental estimates considerably better [34–37]. The greatest difference between the calculated and experimental value of $\Delta H^0_{f,298}$ occurs for CCl_4. However, the values of $\Delta H^0_{f,298}$ obtained by the latter method are closer to experimental estimates for CCl_4 as well as the other reactants and products of the studied reactions. This leads to the conclusion that this method is the most suitable approach in calculations of the enthalpy of formation of chlorine-containing species.

The reaction enthalpy was calculated directly from the total G3-energy of the reactants and products. The calculated values of reaction enthalpy do not depend on the method used to calculate the enthalpy of formation. Figure 2 shows that all investigated reactions are highly endothermic processes. The reaction enthalpy $\Delta H^0_{r,298}$ of 107.1 kJmol^{-1} calculated at the G3 level for reaction $CH_3Cl+Cl \leftrightarrow CH_3+Cl_2$ at room temperature is in excellent agreement with the experimental value of 107.1±0.9 kJmol^{-1} [7]. The theoretical value of $\Delta H^0_{r,298}$ of 92.9 kJmol^{-1} for CH_2Cl_2+

Table 3 Comparison of experimental $\Delta H^0_{f.298}$ (exp.) and theoretical $\Delta H^0_{f.298}$ (calc.) values of the enthalpy of formation of the reactants and products of the studied reactions obtained at the G3 level

Molecular system	$\Delta H^0_{f.298}$ (calc.) (kJmol^{-1})		$\Delta H^0_{f.298}$ (exp.) (kJmol^{-1})[c]
	Formation reaction of CH_xCl_y [a]	Atomization reaction[b]	
CH_3Cl	−80.6	−81.1	−82.0±0.7
CH_2Cl_2	−95.9	−93.0	−95.4±2.5
$CHCl_3$	−108.7	−102.5	−103.3±1.3
CCl_4	−112.1	−102.5	−95.8±2.5
CH_3	145.4	142.6	146.4±0.3
CH_2Cl	115.9	116.4	117.3±3.1
$CHCl_2$	87.1	91.0	89.0±3.0
CCl_3	64.0	71.2	71.1±2.5
Cl	118.9		121.301±0.008

[a] Calculated from G3-energy for the formation reaction of CH_xCl_y from the elemental reference compounds

[b] Calculated from G3-energy for the atomization reaction of CH_xCl_y

[c] From Ref. [7] and papers cited therein

Cl ↔ CH_2Cl+Cl_2 is also very close to that of 91.4±5.6 kJmol^{-1} [7] derived from the experimentally estimated values of $\Delta H^0_{f,298}$ of the reactants and products.

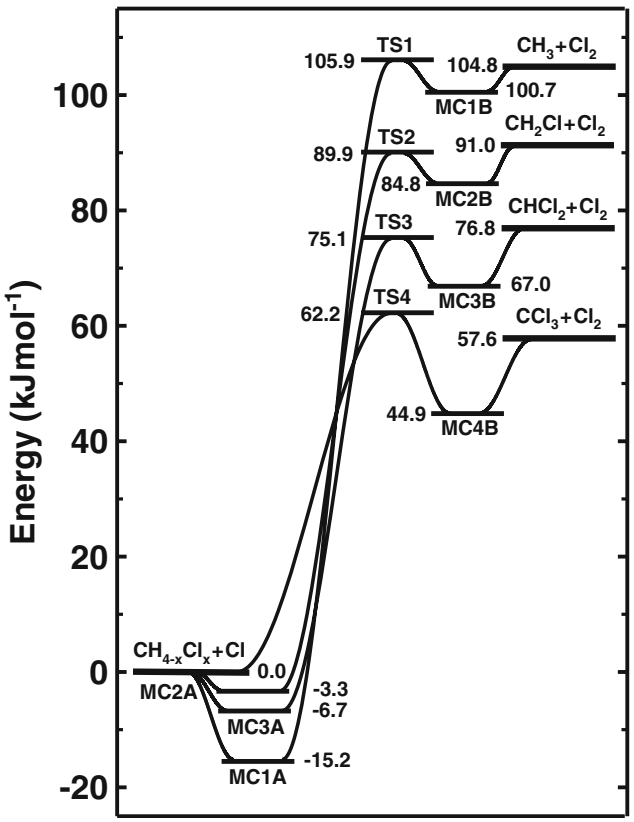

Fig. 2 Schematic profiles of the potential energy surfaces for Cl-abstraction reactions from CH_3Cl, CH_2Cl_2, $CHCl_3$ and CCl_4 by atomic chlorine

In the case of the reaction $CHCl_3+Cl \leftrightarrow CHCl_2+Cl_2$, the calculated value of $\Delta H^0_{r,298}$ of 77.0 kJmol^{-1} at 298 K is 6 kJmol^{-1} higher than the experimental estimate [7]. A more visible difference between the calculated and experimental values of $\Delta H^0_{r,298}$ occurs for $CCl_4+Cl \leftrightarrow CCl_3+Cl_2$. The calculated heat of this reaction of 57.2 kJmol^{-1} distinctly overestimates the experimental value of 45.6 kJmol^{-1} [7] derived at room temperature. This is due to the sizable difference between the theoretical and experimental values of the enthalpy of formation of CCl_4.

Reaction mechanism

The mechanism of the reactions under investigation appears to be complex and consists of some consecutive elementary processes related with the formation of loosely bound intermediate complexes. The profiles of the potential energy surface are shown in Fig. 2. All reactions studied are highly endothermic. Except for reaction CCl_4+Cl, the mechanism of Cl-abstraction proceeds in accordance with a three-step reaction mechanism

$$CH_{4-x}Cl_x + Cl \leftrightarrows CH_{4-x}Cl_x \ldots Cl \leftrightarrows CH_{4-x}Cl_{x-1} \ldots Cl_2 \quad (4)$$
$$\rightarrow CH_{4-x}Cl_{x-1} + Cl_2$$

where x=1,2 and 3. The first and third elementary processes are recombination and unimolecular dissociation, while the second is related to an energy barrier. The pre-reaction adducts formed in the first elementary step are loose molecular complexes. The most stable structure is the adduct $CH_3Cl\ldots Cl$ denoted as MC1A. Its dissociation energy to reactants is 15.2 kJmol^{-1}. The other pre-reaction complexes are considerably less bonded. The next elementary step leads, via TSx, to the molecular complex MCxB, which dissociates to the final channel products, $CH_{4-x}Cl_{x-1}+Cl_2$. The calculated energy barriers for the second step are high, which implies small values of the rate constants for the studied reactions at ambient temperature. It is interesting that the height of the energy barrier is very close to the reaction heat, and both decrease as the number of chlorine atoms in the reactant molecule increases.

In the case of the reactions CCl_4+Cl, the Cl-abstraction process requires only two elementary steps as

$$CCl_4 + Cl \leftrightarrows CCl_3 \ldots Cl_2 \rightarrow CCl_3 + Cl_2 \quad (5)$$

The intermediate complex, $CCl_3\ldots Cl_2$ denoted as MC4B formed in the first elementary step dissociates into the final reaction products, trichloromethyl radical CCl_3 and molecular chlorine Cl_2. The energy barrier for this reaction of 62.2 kJmol^{-1} is the lowest among the reactions studied. Therefore, the reaction CCl_4+Cl should be the fastest process among the reactions under investigation.

Rate constant calculations

There are some theoretical kinetic models for describing the kinetics of a bimolecular reaction, which involve the formation of intermediate molecular complexes [21, 38, 39]. Assuming that the intermediates formed are loosely bound complexes, their collisional stabilization can, at a first approximation, be omitted in the description of the reaction rate. A method for the rate constant calculation for a bimolecular reaction that proceeds through the formation of pre- (MCxA) and post-reaction (MCxB) complexes has been applied successfully to describe the kinetics of many H-abstraction reactions [21–23]. The general equation, which takes into account the rotational energy, is derived from RRKM theory. According to this formalism, the rate coefficient k for the three-step reaction mechanism, such as for Eq. (4) with formation of the pre-reaction and post-reaction adducts, can be expressed as

$$k = \frac{z}{\hbar Q_{RCl} Q_{Cl}} \int_{V_{TSx}}^{\infty} \sum_{J} W_{MCxA}(E,J) \times \frac{W_{TSx}(E,J)}{W_{MCxA}(E,J)+W_{TSx}(E,J)} \times \frac{W_{MCxB}(E,J)}{W_{MCxB}(E,J)+W_{TSx}(E,J)} \times \exp(-E/RT)dE \quad (6)$$

where Q_{RCl} and Q_{Cl} are the partition functions of chloromethane $CH_{4-x}Cl_x$ (x=1,2,3 and 4) and atomic chlorine, respectively, with the center of mass partition function factored out of the product $Q_{RCl}Q_{Cl}$ and included in z together with the partition functions of those inactive degrees of freedom that are not considered by the sums of the states under the integral. V_{TSx} is the threshold energy towards the reactants $CH_{4-x}Cl_x$+Cl, whereas $W_{TSx}(E,J)$, $W_{MCxA}(E,J)$, and $W_{MCxB}(E,J)$ denote the sum of the states at energy less than or equal to E and with angular momentum J for the transition state TSx and the activated complexes for the unimolecular dissociations of MCxA and MCxB, respectively. All computational effort is then related to calculating the sum of the states, $W(E,J)$ This calculation depends on the level at which the conservation of angular momentum is considered and is discussed in detail in Refs. [21, 22].

Equation 6 can be used directly in the description of kinetics of the reactions CH_3Cl+Cl, CH_2Cl_2+Cl and $CHCl_3$+Cl. In the case of the two-step mechanism such as for the reaction CCl_4+Cl , one must replace $W_{MC4A}(E,J)$ by $W_{TS4}(E,J)$ and omit the first fraction under the integral in Eq. (6).

The results of direct calculations [13, 20–22] show that the dominant contribution to the rate constant is given by states with energy E not higher than V_{TSx}+3RT. In the case of a sizable (compared with RT) energy barrier V_{TSx}, the value of the product of the microcanonical branching fractions at an energy slightly higher than V_{TSx} becomes close to unity and the TST rate constant k_{TST} is then a good approximation of the exact rate coefficient, especially at ambient temperatures [13, 20–22].

Reaction system CH_3Cl+Cl

The values of the calculated rate constants are given in Table 4. The height of the energy barrier is clearly the major factor determining the magnitude of the rate constant and its dependence on temperature. Figure 2 shows that the Cl-abstraction from CH_3Cl by Cl atoms is related with a high energy barrier of 106 kJmol^{-1}. The calculated value of the rate constant at 298 K is of 4.5×10^{-30} cm^{3}molecule^{-1}s^{-1}. This value is 17 orders of magnitude lower than the rate constant for the competitive reaction of H-abstraction from CH_3Cl by atomic chlorine [40]. This is the major reason of the lack of experimental measurements of rate constants for Cl-abstraction from CH_3Cl. The kinetics of the reverse reaction CH_3+Cl_2 are considerably better recognized [4–6]. The values of the rate constant for this reaction calculated via the equilibrium constant obtained theoretically are also given in Table 4. The values of the rate constants, k(CH_3Cl+Cl) and k(CH_3+Cl_2) calculated in the temperature range of 200–3,000 K, can be expressed as:

$$k(CH_3Cl + Cl) = 2.08 \times 10^{-11} \times (T/300)^{1.63} \times \exp(-12780/T.) \quad \text{cm}^3\text{molecule}^{-1}\text{s}^{-1} \quad (7)$$

$$k(CH_3 + Cl_2) = 6.70 \times 10^{-13} \times (T/300)^{1.51} \times \exp(270/T) \quad \text{cm}^3\text{molecule}^{-1}\text{s}^{-1} \quad (8)$$

The calculated values of k(CH_3+Cl_2) are compared with available experimental results in Fig. 3. The inset shows the temperature dependence of the calculated k(CH_3Cl+Cl). The room temperature value of the rate constant k (CH_3Cl+Cl) is very low: 2.0×10^{-24} cm^{3}molecule^{-1}s^{-1}. However, the values of k(CH_3Cl+Cl) depend strongly on temperature. The increase in temperature from 200 K to 1,000 K results in a rise in the value of k(CH_3Cl+Cl) by over 20 orders of magnitude. The calculated values of k(CH_3Cl+Cl) are 4.7×10^{-16} and 1.1×10^{-11} cm^{3}molecule^{-1}s^{-1} at 1,000 K and 3,000 K, respectively.

The reverse reaction has been studied experimentally over a wide temperature range. Figure 3 compares our calculated values of k(CH_3+Cl_2) with the experimental results of Eskola et al. [41] performed in the range of 188–500 K, Timonen et al. [42] at 298–423 K, Timonen and Gutman [43] at 296–712 K, and those of Kovalenko and Leone [44] studied at 298 K. The results of Timonen et al. [42] are distinctly underestimated. The other experimental measurements are consistent and show only little dispersion. The calculated values of k(CH_3+Cl_2) can be considered the best compromise between

Table 4 Rate constant calculated for the Cl-abstraction reactions $CH_{4-x}Cl_x+Cl \rightarrow CH_{4-x}Cl_{x-1}+Cl_2$ and their reverse processes

T	$CH_3Cl+Cl \leftrightarrow CH_3+Cl_2$				$CH_2Cl_2+Cl \leftrightarrow CH_2Cl+Cl_2$			
(K)	$k(CH_3Cl+Cl)$ ($cm^3molecule^{-1}s^{-1}$)	$k_{TST}(CH_3Cl+Cl)$ ($cm^3molecule^{-1}s^{-1}$)	$logK_p$	$k(CH_3+Cl_2)$ ($cm^3molecule^{-1}s^{-1}$)	$k(CH_2Cl_2+Cl)$ ($cm^3molecule^{-1}s^{-1}$)	$k_{TST}(CH_2Cl_2+Cl)$ ($cm^3molecule^{-1}s^{-1}$)	$logK_p$	$k(CH_2Cl+Cl_2)$ ($cm^3molecule^{-1}s^{-1}$)
200	2.21×10^{-39}	2.44×10^{-39}	−26.8131	1.39×10^{-12}	2.60×10^{-35}	3.24×10^{-35}	−22.0543	2.83×10^{-13}
250	9.42×10^{-34}	1.02×10^{-33}	−21.2130	1.51×10^{-12}	1.73×10^{-30}	2.00×10^{-30}	−17.2029	2.70×10^{-13}
298	4.49×10^{-30}	4.81×10^{-30}	−17.5717	1.65×10^{-12}	2.42×10^{-27}	2.70×10^{-27}	−14.0551	2.71×10^{-13}
300	5.90×10^{-30}	6.31×10^{-30}	−17.4547	1.66×10^{-12}	3.06×10^{-27}	3.41×10^{-27}	−13.9541	2.71×10^{-13}
350	3.26×10^{-27}	3.48×10^{-27}	−14.7538	1.83×10^{-12}	6.72×10^{-25}	7.40×10^{-25}	−11.6244	2.80×10^{-13}
400	3.92×10^{-25}	4.18×10^{-25}	−12.7171	2.03×10^{-12}	3.98×10^{-23}	4.38×10^{-23}	−9.8716	2.95×10^{-13}
450	1.69×10^{-23}	1.81×10^{-23}	−11.1257	2.24×10^{-12}	9.79×10^{-22}	1.09×10^{-21}	−8.5049	3.12×10^{-13}
500	3.53×10^{-22}	3.81×10^{-22}	−9.8479	2.48×10^{-12}	1.29×10^{-20}	1.46×10^{-20}	−7.4096	3.32×10^{-13}
600	3.56×10^{-20}	3.94×10^{-20}	−7.9238	2.98×10^{-12}	6.48×10^{-19}	7.57×10^{-19}	−5.7646	3.77×10^{-13}
700	1.01×10^{-18}	1.15×10^{-18}	−6.5450	3.53×10^{-12}	1.10×10^{-17}	1.34×10^{-17}	−4.5896	4.28×10^{-13}
800	1.28×10^{-17}	1.51×10^{-17}	−5.5099	4.13×10^{-12}	9.39×10^{-17}	1.20×10^{-16}	−3.7099	4.82×10^{-13}
900	9.40×10^{-17}	1.15×10^{-16}	−4.7054	4.77×10^{-12}	5.06×10^{-16}	6.80×10^{-16}	−3.0280	5.41×10^{-13}
1000	4.70×10^{-16}	5.96×10^{-16}	−4.0630	5.44×10^{-12}	1.97×10^{-15}	2.78×10^{-15}	−2.4848	6.03×10^{-13}
1500	6.44×10^{-14}	9.90×10^{-14}	−2.1559	9.26×10^{-12}	1.24×10^{-13}	2.21×10^{-13}	−0.8807	9.50×10^{-13}
2000	8.01×10^{-13}	1.48×10^{-12}	−1.2290	1.37×10^{-11}	1.04×10^{-12}	2.27×10^{-12}	−0.1083	1.35×10^{-12}
2500	3.73×10^{-12}	8.10×10^{-12}	−0.6918	1.85×10^{-11}	3.85×10^{-12}	9.96×10^{-12}	0.3353	1.79×10^{-12}
3000	1.05×10^{-11}	2.65×10^{-11}	−0.3470	2.35×10^{-11}	9.31×10^{-12}	2.81×10^{-11}	0.6173	2.26×10^{-12}

T	$CHCl_3+Cl \leftrightarrow CHCl_2+Cl_2$				$CCl_4+Cl \leftrightarrow CCl_3+Cl_2$			
(K)	$k(CHCl_3+Cl)$ ($cm^3molecule^{-1}s^{-1}$)	$k_{TST}(CHCl_3+Cl)$ ($cm^3molecule^{-1}s^{-1}$)	$logK_p$[a]	$k(CHCl_2+Cl_2)$ ($cm^3molecule^{-1}s^{-1}$)	$k(CCl_4+Cl)$ ($cm^3molecule^{-1}s^{-1}$)	$k_{TST}(CCl_4+Cl)$ ($cm^3molecule^{-1}s^{-1}$)	$logK_p$	$k(CCl_3+Cl_2)$ ($cm^3molecule^{-1}s^{-1}$)
200	4.41×10^{-31}	4.41×10^{-31}	−16.1416	6.10×10^{-15}	1.67×10^{-27}	1.68×10^{-27}	−12.4458	5.75×10^{-15}
250	4.64×10^{-27}	4.66×10^{-27}	−12.3986	1.16×10^{-14}	3.87×10^{-24}	3.91×10^{-24}	−9.4180	1.21×10^{-14}
298	1.98×10^{-24}	2.00×10^{-24}	−9.9802	1.89×10^{-14}	6.18×10^{-22}	6.29×10^{-22}	−7.4703	2.11×10^{-14}
300	2.41×10^{-24}	2.43×10^{-24}	−9.9033	1.92×10^{-14}	7.28×10^{-22}	7.41×10^{-22}	−7.4080	2.16×10^{-14}
350	2.20×10^{-22}	2.25×10^{-22}	−8.1223	2.91×10^{-14}	3.20×10^{-20}	3.30×10^{-20}	−5.9800	3.48×10^{-14}
400	6.73×10^{-21}	6.97×10^{-21}	−6.7878	4.13×10^{-14}	5.65×10^{-19}	5.92×10^{-19}	−4.9152	5.20×10^{-14}
450	9.87×10^{-20}	1.04×10^{-19}	−5.7513	5.57×10^{-14}	5.37×10^{-18}	5.74×10^{-18}	−4.0921	7.34×10^{-14}
500	8.61×10^{-19}	9.25×10^{-19}	−4.9239	7.23×10^{-14}	3.30×10^{-17}	3.61×10^{-17}	−3.4379	9.91×10^{-14}
600	2.30×10^{-17}	2.58×10^{-17}	−3.6873	1.12×10^{-13}	5.16×10^{-16}	5.95×10^{-16}	−2.4664	1.63×10^{-13}
700	2.46×10^{-16}	2.91×10^{-16}	−2.8095	1.59×10^{-13}	3.76×10^{-15}	4.59×10^{-15}	−1.7824	2.44×10^{-13}
800	1.49×10^{-15}	1.85×10^{-15}	−2.1559	2.13×10^{-13}	1.68×10^{-14}	2.19×10^{-14}	−1.2768	3.39×10^{-13}
900	6.10×10^{-15}	8.02×10^{-15}	−1.6519	2.74×10^{-13}	5.45×10^{-14}	7.58×10^{-14}	−0.8895	4.47×10^{-13}
1000	1.90×10^{-14}	2.64×10^{-14}	−1.2523	3.39×10^{-13}	1.40×10^{-13}	2.08×10^{-13}	−0.5844	5.66×10^{-13}
1500	6.02×10^{-13}	1.09×10^{-12}	−0.0859	7.34×10^{-13}	2.39×10^{-12}	4.96×10^{-12}	0.2925	1.27×10^{-12}
2000	3.49×10^{-12}	8.02×10^{-12}	0.4641	1.20×10^{-12}	9.71×10^{-12}	2.77×10^{-11}	0.6943	2.02×10^{-12}
2500	1.01×10^{-11}	2.87×10^{-11}	0.7732	1.71×10^{-12}	2.19×10^{-11}	8.38×10^{-11}	0.9135	2.74×10^{-12}
3000	2.06×10^{-11}	7.08×10^{-11}	0.9652	2.23×10^{-12}	3.69×10^{-11}	1.85×10^{-10}	1.0450	3.40×10^{-12}

[a] The equilibrium constant K_p calculated for the reaction enthalpy corrected by $-6.0\ kJmol^{-1}$ to obtain value of $\Delta H^0_{f.298}$ of $71.0\ kJmol^{-1}$ (see text)

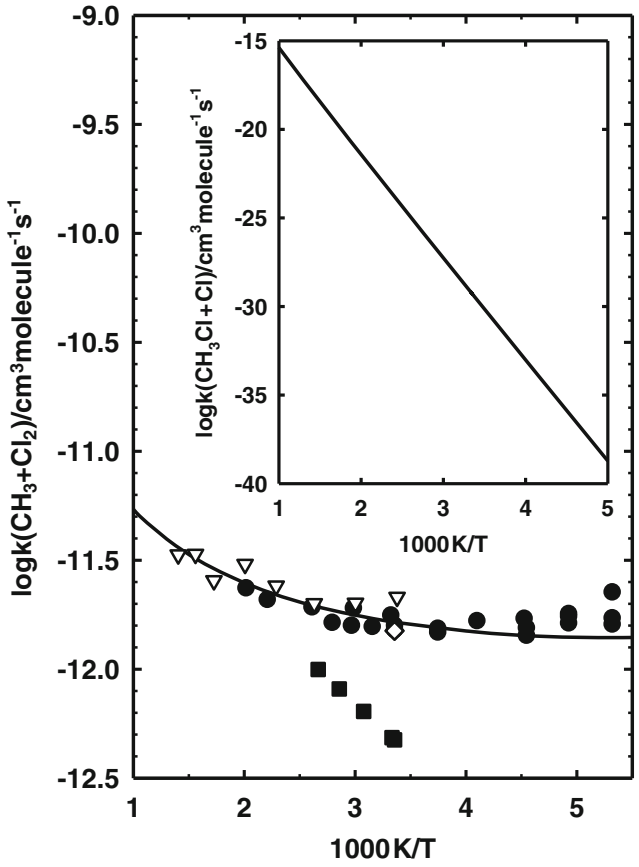

Fig. 3 Arrhenius plot for the reaction $CH_3+Cl_2 \rightarrow CH_3Cl+Cl$ comparing the available results of kinetic measurements of Eskola et al. [41] (*black circles*), Timonen et al. [42] (*black squares*), Timonen and Gutman [43] (*white triangles*), and Kovalenko and Leone [44] (*white diamonds*) with those obtained theoretically in this study. *Solid line* Plot of Eq. (8). *Inset* Temperature dependence of $k(CH_3Cl+Cl)$ from Eq. (7)

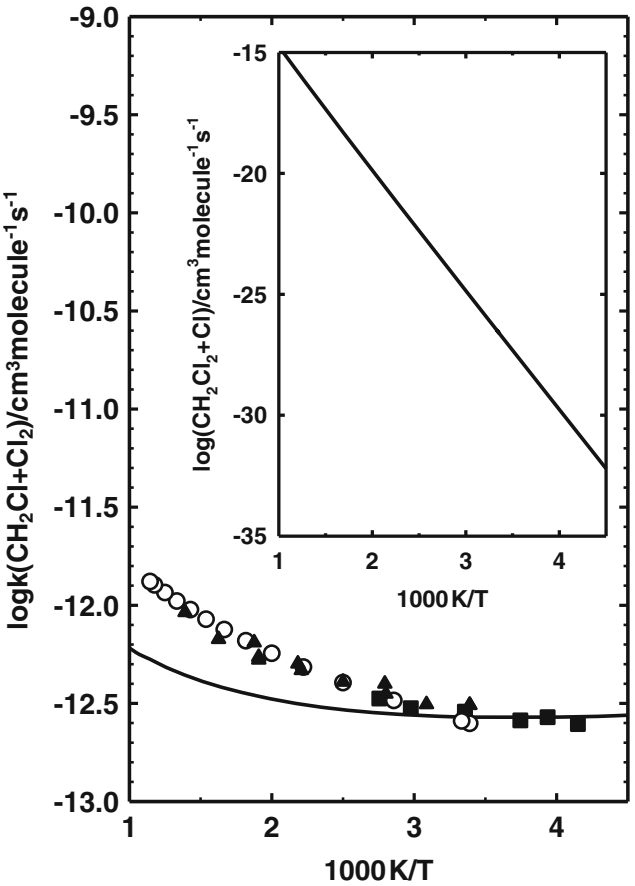

Fig. 4 Arrhenius plot for the reaction $CH_2Cl+Cl_2 \rightarrow CH_2Cl_2+Cl$ comparing the available results of kinetic measurements of Seetula [45] (*white circles*), Seetula et al. [46] (*black triangles*) and Eskola et al. [47] by (*black squares*) with those obtained theoretically in this study. *Solid line* Plot of Eq. (10). *Inset* Temperature dependence of $k(CH_2Cl_2+Cl)$ from Eq. (9)

the available estimates. The predicted temperature dependence of the rate constants, $k(CH_3Cl+Cl)$ and $k(CH_3+Cl_2)$ expressed by Eqs. (7) and (8) allows a description of the kinetics of the reactions CH_3Cl+Cl and CH_3+Cl_2 over a wide temperature range.

Reaction system CH_2Cl_2+Cl

The profiles of the potential energy surface presented in Fig. 2 show that Cl abstraction from CH_2Cl_2 by Cl atoms is also related to a high energy barrier of 90 kJmol^{-1}. This implies a low values of the rate constants $k(CH_2Cl_2+Cl)$. The calculated value of $k(CH_2Cl_2+Cl)$ at 298 K of 2.4×10^{-27} cm^{3}molecule^{-1} s^{-1} is over 1,000 times higher than the value of $k(CH_3Cl+Cl)$ at the same temperature. The height of the energy barrier is lower by 16 kJmol^{-1} than that calculated for CH_3Cl+Cl. As a consequence, values of $k(CH_2Cl_2+Cl)$ increase a little more weakly with temperature than values of $k(CH_3Cl+Cl)$. The calculated values of $k(CH_2Cl_2+Cl)$ are 2.0×10^{-15} and 9.3×10^{-12} cm^{3}molecule^{-1}s^{-1} at 1,000 K and 3,000 K, respectively. To the best of our knowledge there is no experimental information on the kinetics of CH_2Cl_2+Cl. However, the reverse reaction CH_2Cl+Cl_2 has been studied experimentally [45–47] in the temperature range 201–873 K. Figure 4 compares our theoretical results with the results of the experimental investigations of Seetula [45], Seetula et al. [46] and Eskola et al. [47] obtained for CH_2Cl+Cl_2. The values of the rate constants, $k(CH_2Cl_2+Cl)$ and $k(CH_2Cl+Cl_2)$ calculated in the temperature range of 200–3,000 K, can be expressed as

$$k(CH_2Cl_2+Cl) = 2.36\times10^{-11}\times(T/300)^{1.23}\times\exp(-10960/T) \quad \text{cm}^3\text{molecule}^{-1}\text{s}^{-1} \tag{9}$$

$$k(CH_2Cl+Cl_2) = 7.34\times10^{-14}\times(T/300)^{1.43}\times\exp(390/T) \quad \text{cm}^3\text{molecule}^{-1}\text{s}^{-1} \tag{10}$$

The results of our calculations reproduce the experimentally estimated values of $k(CH_2Cl+Cl_2)$ very well at low

temperatures, i.e., below 400 K. At higher temperatures, our values of $k(CH_2Cl+Cl_2)$ are slightly lower compared with the experimental results. The difference between the experimental and theoretical results increases with increasing temperature. The experimental value of $(9.22\pm0.54)\times10^{-13}$ $cm^3molecule^{-1}s^{-1}$ obtained by Seetula et al. [46] at 719 K is two times higher than the 4.4×10^{-13} $cm^3molecule^{-1}s^{-1}$ derived from Eq. (10). This may be an effect of the treatment of the lowest degrees of freedom of the transition state TS2 as harmonic vibrations. However, it should be emphasized that the theoretically derived values of $k(CH_2Cl+Cl_2)$ and $k(CH_2Cl_2+Cl)$ describe very well the kinetics of the chlorine abstraction reactions CH_2Cl_2+Cl and CH_2Cl+Cl_2 at temperatures not higher than ambient.

Reaction system $CHCl_3+Cl$

The calculated energy barrier of 75 $kJmol^{-1}$ for reaction $CHCl_3+Cl$ is lower by 15 and 31 $kJmol^{-1}$ than those derived for CH_2Cl_2+Cl and CH_3Cl+Cl, respectively. This indicates that chlorine abstraction proceeds more easily from a reactant with a greater number of chlorine atoms. The height of the energy barrier for chlorine abstraction decreases by 15 kJ mol^{-1} for any subsequent chlorine atom inserted into the chloromethane molecule. However, the energy barrier for $CHCl_3+Cl$ is still high, which implies a low value of the rate constant $k(CH_2Cl_2+Cl)$ at room temperature. The calculated value of $k(CH_2Cl_2+Cl)$ at 298 K is of 2.0×10^{-24} cm^3 $molecule^{-1}s^{-1}$. This value is over 3 and 6 orders of magnitude higher than the calculated at the same temperature values of $k(CH_3Cl+Cl)$ and $k(CH_2Cl_2+Cl)$, respectively. The derived temperature dependence of $k(CHCl_3+Cl)$ can be expressed in the temperature range 200–3,000 K as,

$$k(CHCl_3+Cl) = 5.28\times10^{-11}\times(T/300)^{0.97}\times\exp(-9200/T)\quad cm^3molecule^{-1}s^{-1} \tag{11}$$

According to the sizable energy barrier, the reaction $CHCl_3+Cl$ becomes important only at very high temperatures. Experimental information is available only for the reverse process, $CHCl_2+Cl_2$ [45, 46]. Figure 5 shows a comparison of the temperature dependence of the rate constant $k(CHCl_2+Cl_2)$ derived theoretically with that from experimental findings [45, 46]. The dashed line denotes the values of the rate constant $k(CHCl_2+Cl_2)$ obtained *via* the calculated equilibrium constant. The calculated values of $k(CHCl_2+Cl_2)$ distinctly overestimate the experimental results of Seetula [45] and Seetula et al. [46], especially at low temperatures.

It is worth noting that a comparison of the theoretical and experimental values of $k(CHCl_2+Cl_2)$ is indeed the only way to verify, albeit indirectly, the calculated values of both $k(CHCl_2+Cl_2)$ and $k(CHCl_3+Cl)$, on the condition that the calculated equilibrium constants are realistic. The calculated reaction

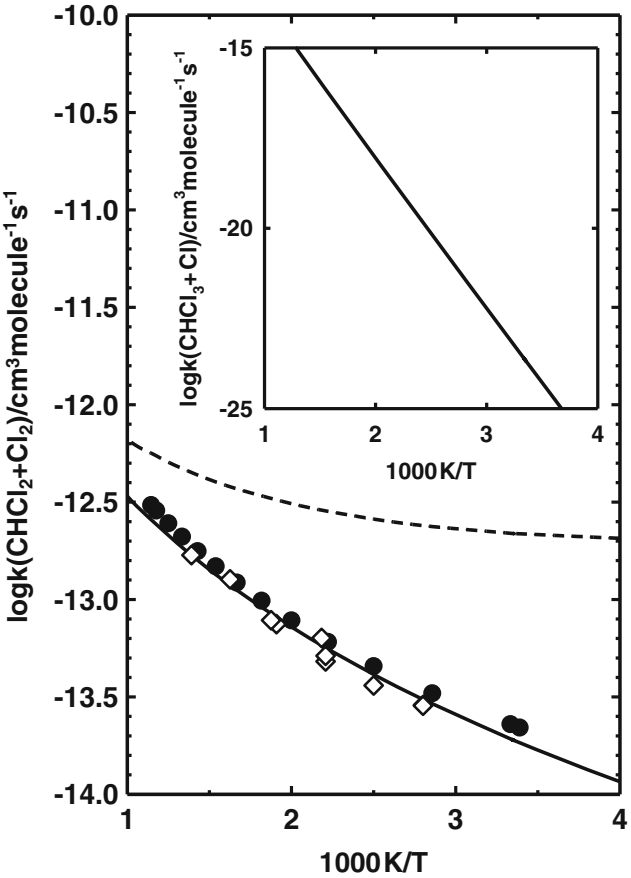

Fig. 5 Arrhenius plot for the reaction $CHCl_2+Cl_2\rightarrow CHCl_3+Cl$ comparing the available results of kinetic measurements of Seetula [45] (*black circles*) and Seetula et al. [46] (*white diamonds*) with those obtained theoretically in this study. The *dashed* and *solid curves* show the temperature dependence of $k(CHCl_2+Cl_2)$ derived from the values of the rate constant $k(CHCl_3+Cl)$ and the equilibrium constant corresponding to the reaction enthalpy at room temperature of 77.0 and 71.0 $kJmol^{-1}$ (see text), respectively. *Inset* Temperature dependence of $k(CHCl_3+Cl)$ from Eq. (11)

enthalpy at room temperature for $CHCl_3+Cl\rightarrow CHCl_2+Cl_2$ is of 77.0 $kJmol^{-1}$, whereas the experimentally estimated one is 71.0 $kJmol^{-1}$ [7]. The correction of the reaction enthalpy by −6.0 $kJmol^{-1}$ at any temperature should lead to more realistic values of the equilibrium constant, and finally to a more reliable rate constant $k(CHCl_2+Cl_2)$. The values of $k(CHCl_2+Cl_2)$ after reduction by a factor of exp(6.0 $kJmol^{-1}$/RT), shown in Fig. 5 (solid line), can be expressed by

$$k(CHCl_2+Cl_2) = 6.81\times10^{-14}\times(T/300)^{1.60}\times\exp(-370/T)\quad cm^3molecule^{-1}s^{-1} \tag{12}$$

The corrected values of the rate constant, $k(CHCl_2+Cl_2)$ reproduce the experimental results very well. Agreement between experimental and calculated values of $k(CHCl_2+Cl_2)$ is excellent over a wide temperature range. This also confirms the reliability of the values of the rate constant, $k(CHCl_3+Cl)$ calculated in this study.

Reaction system CCl_4+Cl

Figure 2 shows that the lowest energy barrier of 62 kJmol^{-1} was found for the reaction of CCl_4+Cl. The calculated value of $k(CCl_4+Cl)$ of 6.2×10^{-22} cm^{3}molecule^{-1}s^{-1} at 298 K is over 300 times higher than the value of $k(CHCl_3+Cl)$ at the same temperature (see Table 4). The sizable energy barrier for CCl_4+Cl results in the distinct temperature dependence of $k(CCl_4+Cl)$. The values of $k(CCl_4+Cl)$ and $k(CCl_3+Cl_2)$ for the reverse reaction calculated via the equilibrium constant can be expressed in the form

$$k(CCl_4+Cl) = 1.51\times10^{-10}\times(T/300)^{0.58}\times\exp(-7790/T) \quad cm^3molecule^{-1}s^{-1} \tag{13}$$

$$k(CCl_3+Cl_2) = 1.43\times10^{-13}\times(T/300)^{1.52}\times\exp(-550/T) \quad cm^3molecule^{-1}s^{-1} \tag{14}$$

The kinetics of reaction CCl_4+Cl have been studied experimentally by Seetula [45] and DeMare and Huybrechts [48]. Their investigations were, however, performed in different temperature ranges, and the reported temperature dependencies of $k(CCl_4+Cl)$ expressed in the Arrhenius' form show distinct differences in both the pre-exponential factor and the activation energy, which makes it difficult to compare the experimental and theoretical values of $k(CCl_4+Cl)$. There is no experimental information on the kinetics of the reverse reaction CCl_3+Cl_2. The reaction CCl_4+Cl is one of the processes involved in the pyrolysis of CCl_4 in the gas-phase. Huybrechts et al. [49] studied the pyrolysis of CCl_4 in terms of modeling by computer simulations and optimizations of the kinetic parameters of the elementary processes taking part in the mechanism of the investigated pyrolysis. The Arrhenius parameters derived from the kinetic model of Huybrechts et al. [49] allow a description of the kinetics of the reaction CCl_4+Cl in the temperature range 300–800 K. The value of 4.9×10^{-22} cm^{3}molecule^{-1}s^{-1} derived at 300 K by Huybrechts et al. [49] is lower than our estimate of 7.3×10^{-22} cm^{3}molecule^{-1}s^{-1}. The similar difference between our result for the value of $k(CCl_4+Cl)$ and that derived by Huybrechts et al. [49] is maintained at temperatures below 800 K. This agreement can be considered as satisfactory taking into account the uncertainties of the kinetic modeling procedure.

Summary

The main aim of the present study was to perform a theoretical analysis of the kinetics of chlorine abstraction from chlorinated methanes, CH_3Cl, CH_2Cl_2, $CHCl_3$ and CCl_4 by chlorine atoms. Theoretical investigations based on ab initio calculations of the $CH_{4-x}Cl_x+Cl\rightarrow CH_{4-x}Cl_{x-1}+Cl_2$ (x= 1,2,3 and 4) reaction systems at the G3 level were performed to gain insight into the reaction mechanism. Kinetic information on these reactions is very limited. The results of the calculations also allow an estimation of the reaction energetics and the molecular properties of the structures taking part in the reaction mechanism.

The calculated values of the enthalpy of formation of the reactants and products are in good agreement with the reported values estimated experimentally. All the studied reactions are strongly endothermic processes, with calculated values of reaction enthalpy at 298 K of 107.1, 92.9, 77.0 and 57.2 kJmol^{-1} for CH_3Cl+Cl, CH_2Cl_2+Cl, $CHCl_3$+Cl and CCl_4+Cl, respectively. The calculated profiles of the potential energy surface show that the mechanism of the reactions studied is complex and that Cl-abstraction proceeds via the formation of intermediate complexes. The multi-step reaction mechanism consists of two elementary steps in the case of CCl_4+Cl, and three steps for the other reactions. The heights of the energy barrier relative to the Cl-abstraction by Cl atoms from CH_3Cl, CH_2Cl_2, $CHCl_3$ and CCl_4 are 106, 90, 75 and 62 kJmol^{-1}, respectively. The differences in energy barriers are reflected in the values of the rate constants. The rate constants calculated at 298 K are 4.5×10^{-30}, 2.4×10^{-27}, 2.0×10^{-24} and 6.2×10^{-22} cm^{3}molecule^{-1}s^{-1} for reactions $CH_3Cl/CH_2Cl_2/CHCl_3/CCl_4$+Cl, respectively. The rate constants for the reverse reactions $CH_3/CH_2Cl/CHCl_2/CCl_3+Cl_2$ have also been calculated using the equilibrium constants derived theoretically. The ordering of the values of the calculated rate constants for the reverse reactions is quite the opposite of their counterparts in the forward direction. The highest value of 1.7×10^{-12} cm^{3}molecule^{-1}s^{-1} at 298 K is found for $k(CH_3+Cl_2)$, the lowest one is $k(CCl_3+Cl_2) = 2.1\times10^{-14}$ cm^{3}molecule^{-1}s^{-1}. The calculated values of the rate constants describe the kinetics of the reverse reactions well. An especially good agreement between the calculated and reported values of the rate constants was reached for reactions CH_3+Cl_2, CH_2Cl+Cl_2 and $CHCl_2+Cl_2$. In the temperature range of 200–400 K, the theoretically derived kinetic parameters for these reactions allow the reaction kinetics to be described with an accuracy no worse than that given by various kinetic data evaluations.

This confirms the reliability of the theoretically derived kinetic expressions, which represent a substantial supplement to the kinetic data necessary for the description and modeling of the complex gas-phase reactions of importance in combustion and atmospheric chemistry.

Acknowledgments This research was supported by Wroclaw Medical University under grant No. ST-694. The Wroclaw Center of Networking and Supercomputing is acknowledged for the generous allotment of computer time.

References

1. Finnlayson-Pitts BJ, Pitts JN Jr (2000) Chemistry of the upper and lower atmosphere. Academic, San Diego
2. Brasseur GP, Orlando JJ, Tyndall GS (1999) Atmospheric chemistry and global change. Oxford University Press, Oxford
3. Khalil MAK, Rasmussen RA (1999) Atmos Environ 33:1305–1321
4. Keene WC, Khalil MA, Erikson DJ, McCulloch A, Graedel TE, Lobert JM, Aucott ML, Gong SL, Harper DB, Kleiman G, Midgley P, Moore RM, Seuzaret C, Sturges WT, Benkovitz CM, Koropalov V, Barrie LA, Li YF (1999) J Geophys Res 104:8429–8440
5. Prather MJ, Watson RT (1990) Nature 344:729–734
6. Sander SP, Friendl RR, Golden DM, Kurylo MJ, Moorgat GK, Wine PH, Ravishankara AR, Kolb CE, Molina MJ, Finlayson-Pitts BJ, Huie RE, Orkin VL (2006) NASA Panel for data evaluation: chemical kinetics and photochemical data for use in atmospheric studies, evaluation number 15, National Aeronautics and Space Administration, Jet Propulsion Laboratory. California Institute of Technology, Pasadena CA
7. Atkinson R, Baulch DL, Cox RA, Crowley JN, Hampson RF, Hynes RG, Jenkin ME, Rossi MJ, Troe J (2004) Atmos Chem Phys 4:1461–1738
8. Atkinson R, Baulch DL, Cox RA, Crowley JN, Hampson RF, Hynes RG, Jenkin ME, Rossi MJ, Troe J, Wallington TJ (2008) Atmos Chem Phys 8:4141–4496
9. Curtiss LA, Raghavachari K, Trucks GW, Pople JA (1991) J Chem Phys 94:7221–7230
10. Notario R, Castaño O, Abboud JLM (1996) Chem Phys Lett 263:367–370
11. Espinosa-Garcia J (1999) Chem Phys Lett 315:239–247
12. Segovia M, Ventura ON (1997) Chem Phys Lett 277:490–496
13. Brudnik K, Jodkowski JT, Ratajczak E, Venkatraman R, Nowek A, Sullivan RH (2001) Chem Phys Lett 345:435–444
14. Fernández LE, Varetti EL (2003) J Mol Struct (THEOCHEM) 629:175–183
15. Brudnik K, Jodkowski JT, Ratajczak E (2003) J Mol Struct 656:333–339
16. Brudnik K, Jodkowski JT, Ratajczak E (2003) Bull Pol Acad Sci Chem 51:77–91
17. Brudnik K, Jodkowski JT, Nowek A, Leszczynski J (2007) Chem Phys Lett 435:194–200
18. Brudnik K, Wójcik-Pastuszka D, Jodkowski JT, Leszczynski J (2008) J Mol Model 14:1159–1172
19. Brudnik K, Gola AA, Jodkowski JT (2009) J Mol Model 15:1061–1066
20. Brudnik K, Jodkowski JT, Sarzyński D, Nowek A (2011) J Mol Model 17:2395–2409
21. Jodkowski JT, Rayez MT, Rayez JC, Bérces T, Dóbé S (1998) J Phys Chem A 102:9219–9229
22. Jodkowski JT, Rayez MT, Rayez JC, Bérces T, Dóbé S (1998) J Phys Chem A 102:9230–9243
23. Jodkowski JT, Rayez MT, Rayez JC, Bérces T, Dóbé S (1999) J Phys Chem A 103:3750–3765
24. Curtiss LA, Raghavachari K, Redfern PC, Rassolov V, Pople JA (1998) J Chem Phys 109:7764–7776
25. Frisch MJ, Trucks GW, Schlegel HB, Scuseria GE, Robb MA, Cheeseman JR, Scalmani G, Barone V, Mennucci B, Petersson GA, Nakatsuji H, Caricato M, Li X, Hratchian HP, Izmaylov AF, Bloino J, Zheng G, Sonnenberg JL, Hada M, Ehara M, Toyota K, Fukuda R, Hasegawa J, Ishida M, Nakajima T, Honda Y, Kitao O, Nakai H, Vreven T, Montgomery JA Jr, Peralta JE, Ogliaro F, Bearpark M, Heyd JJ, Brothers E, Kudin KN, Staroverov VN, Kobayashi R, Normand J, Raghavachari K, Rendell A, Burant JC, Iyengar SS, Tomasi J, Cossi M, Rega N, Millam JM, Klene M, Knox JE, Cross JB, Bakken V, Adamo C, Jaramillo J, Gomperts R, Stratmann RE, Yazyev O, Austin AJ, Cammi R, Pomelli C, Ochterski JW, Martin R, Morokuma K, Zakrzewski VG, Voth GA, Salvador P, Dannenberg JJ, Dapprich S, Daniels AD, Farkas O, Foresman JB, Ortiz JV, Cioslowski J, Fox DJ (2009) Gaussian 09, Revision A 02. Gaussian Inc, Wallingford
26. Johnston HS (1966) Gas-phase reaction rate theory. Ronald, New York
27. Laidler KJ (1969) Theories of chemical reaction rates. McGraw-Hill, New York
28. Shimanouchi T (1972) Tables of molecular vibrational frequencies, Consolidated vol. I, National Bureau of Standards, NSRDS-NBS 39
29. Herzberg G, Shoosmith J (1956) Can J Phys 34:523–525
30. Jacox ME, Milligan DE (1970) J Chem Phys 53:2688–2701
31. Jacox ME (1998) J Phys Chem Ref Data 27:115–393
32. Jacox ME (2003) J Phys Chem Ref Data 32:1–441
33. Chase MW Jr (1998) J Phys Chem Ref Data Monogr 9:1–1951
34. Ma NL, Lau KC, Chien SH, Li WK (1999) Chem Phys Lett 31:275–280
35. Felmy DA, Tratnyek AR, Bylaska PG, Dixon EJ (2002) 106:11581–11593
36. Csontos J, Rolik Z, Das S, Kallay M (2010) J Phys Chem A 114:13093–13103
37. Zhang J, Zhou W, Li Y, Gao H, Zhou Z (2010) J Fluor Chem 131:606–611
38. Mozurkevich M, Benson SW (1984) J Phys Chem 88:6429
39. Chen Y, Rauk A, Tschuikow-Roux E (1991) J Phys Chem 95:9900
40. Sarzyński D, Gola AA, Andrzej Dryś A, Jodkowski JT (2009) Chem Phys Lett 476:138–142
41. Eskola AJ, Timonen RS, Marshall P, Chesnokov EN, Krasnoperov LN (2008) J Phys Chem A 112:7391–7401
42. Timonen R, Kalliorinne K, Koskikallio J (1986) Acta Chem Scand Ser A 40:459–466
43. Timonen R, Gutman D (1986) J Phys Chem 90:2987–2991
44. Kovalenko LJ, Leone SR (1984) J Chem Phys 80:3656–3667
45. Seetula JA (1998) J Chem Soc Faraday Trans 94:3561–3567
46. Seetula JA, Gutman D, Lightfoot PD, Rayes MT, Senkan SM (1991) J Phys Chem 95:10688–10693
47. Eskola AJ, Geppert WD, Rissanen MP, Timonen RS, Halonen L (2010) J Phys Chem A 114:4805–4810
48. DeMare GR, Huybrechts G (1968) Trans Faraday Soc 64:1311–1318
49. Huybrechts G, Narmon M, Van Mele B (1996) Int J Chem Kinet 28:27–36